Supporting Information

Theory of hysteresis in halide perovskites by integration of the equivalent circuit

Juan Bisquert,* Antonio Guerrero, Cedric Gonzales
Institute of Advanced Materials (INAM), Universitat Jaume I, 12006 Castelló, Spain.

Corresponding author J. Bisquert (bisquert@uji.es)

1. Different polarization schedules

To analyze the hysteresis in CV in the reverse direction for the capacitive circuit we first choose a point at voltage V_1 in the stationary curve that starts at $I(0)=0$. It has the values

$$I_1 = \frac{V_m}{R_{10}+R_{30}}\left(e^{V_1/V_m}-1\right) \tag{1}$$

$$w_{p1} = \frac{r_0}{r_1}V_1 \tag{2}$$

We use this point as the initial condition. We wish to apply a negative sweep velocity (from forward voltage to reverse voltage) that we write as $B_s = -V_s$. We obtain

$$w_p(V,V_1,B_s) = -\frac{r_0}{{r_1}^2}B_s\, e^{r_1/B_s\,(V-V_1)} + \frac{r_0}{r_1}V + \frac{r_0 B_s}{{r_1}^2} \tag{3}$$

$$I(V,V_1,B_s) = \frac{V_m}{R_{10}+R_{30}}\left(e^{V/V_m}-1\right) + \frac{1}{R_{30}}\frac{r_0}{r_1}\frac{B_s}{\frac{B_s}{V_m}+1}\left(e^{V/V_m + r_1/B_s\,(V-V_1)} - e^{V_1/V_m}\right) \tag{4}$$

The reverse scans at progressively large negative velocities (forward voltage to reverse voltage) are shown in Fig. S1. The current at the origin is given by the expression

$$I(0,V_1,B_s) = -\frac{1}{R_{30}}\frac{r_0}{r_1}\frac{B_s}{\frac{B_s}{V_m}+1}\left(e^{V_1/V_m} - e^{-r_1 V_1/B_s}\right) \tag{5}$$

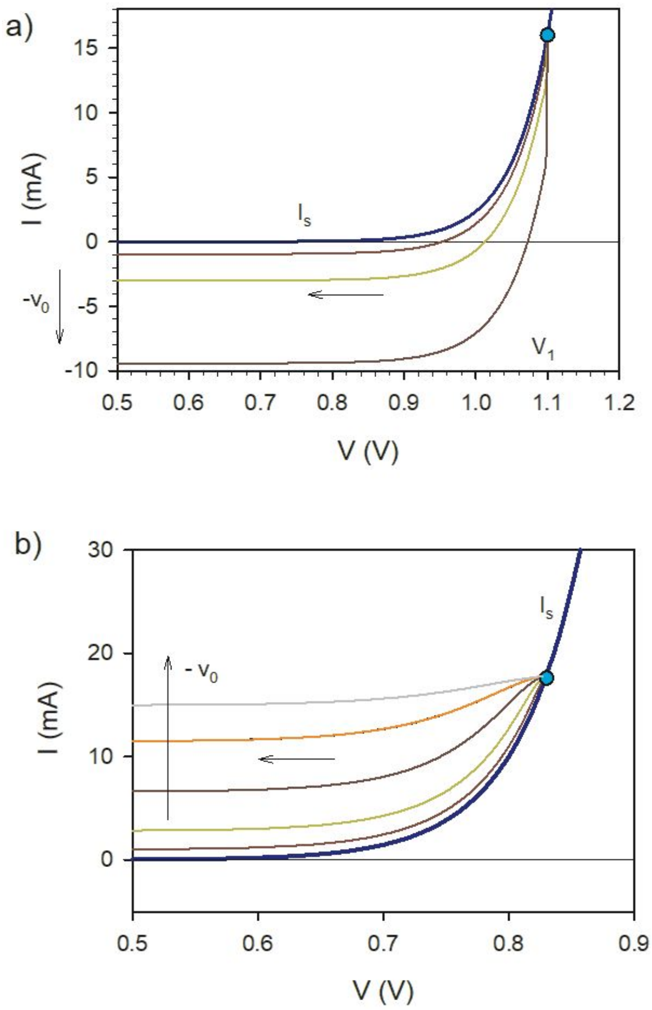

Fig. S1. (a) Current-voltage curves at different reverse scan rates, Eq. (5), for the capacitive circuit with parameters $R_{10} = 1 \times 10^5\ \Omega$, $R_{30} = 49 \times 10^5\ \Omega$, $r_1 = 50$, $\tau_1 = 1$ s, $C_1 = 10^{-5}$ F, $k_B T =$ 0.026 V, $m = 2$, $V_m = 0.052$ V, and the stationary curve. The reverse scan starts at the equilibrium curve at voltage $V_1 = 1.1$ V , indicated by a point. The sweep velocities $V_s = \tau_1 v_0$, are $-v_0 = 10^{-2.5}$, 10^{-2}, $10^{-1.5}$ V/s. (b) Current-voltage curves at different reverse scan rates for the inductive circuit with parameters $R_{dc0} = 2.5 \times 10^4\ \Omega$, $R_{10} = 50/49\ R_{dc0}$, $R_{30} = 50\ R_{dc0}$, $\tau_k = 1$ s, $k_B T =$ 0.026 V, $m = 2$, $V_m = 0.052$ V, and the stationary curve. The reverse scan starts at the equilibrium curve at voltage $V_1 = 0.83$ V , indicated by a point. The sweep velocities $V_s = \tau_1 v_0$, are $-v_0 = 10^{-2.5}$, 10^{-2}, $10^{-1.5}$, 10^{-1} , $10^{-0.5}$, V/s.

In the inductive circuit in the reverse direction for the capacitive circuit the point at voltage V_1 in the stationary curve that starts at $I(0) = 0$ gives

$$I_1 = \frac{V_m}{R_{dc0}}\left(e^{V_1/V_m} - 1\right) \tag{6}$$

In the memory value we allow for a voltage ΔV_1 in excess of the equilibrium value

$$w_{a1} = V_1 + \Delta V_1 \tag{7}$$

We now take V_1 as the initial condition. We apply a negative sweep velocity $B_s = - V_s$. We obtain

$$w_p(V,V_1,B_s) = V + \Delta V_1 - B_s\left[e^{(V - V_1)/B_s} - 1\right] \tag{8}$$

$$I(V,V_1,B_s) = \frac{V_m}{R_{dc0}}\left(e^{V/V_m} - 1\right) + \frac{1}{R_{a0}}\frac{B_s - \Delta V_1}{\frac{B_s}{V_m} + 1}\left(e^{V_1/V_m} - e^{V/V_m + (V - V_1)/B_s}\right) \tag{9}$$

The reverse scans are shown in Fig. S1b. The current at the origin has the value

$$I(0,V_1,B_s) = \frac{1}{R_{a0}}\frac{B_s}{\frac{B_s}{V_m} + 1}\left(e^{V_1/V_m} - e^{-V_1/B_s}\right) \tag{10}$$

Besides the change of the *J-V* curves by the sweep rate, another important hysteretic effect is the modification of *J-V* curves by voltage or light pretreatment that induce polarization. Effects of poling are well known and can increase the performance of the solar cell, or reduce it by the artefact of the depolarization currents.[1-4] To describe these situations we start the forward evolution with initial value w_{a0} in the model for the inductive circuit, Eq. (66). It produces an increase of the negative current discharge as shown in Fig. S2a. In the current-voltage curve under illumination this effect produces the overshoot of the *J-V* curve under illumination. The effect of prepolarization of the memory variable by an amount ΔV_1 in excess of the equilibrium value, in reverse scan from a voltage V_1, is shown in Fig. S2b. These effects have been discussed previously.[5-7]

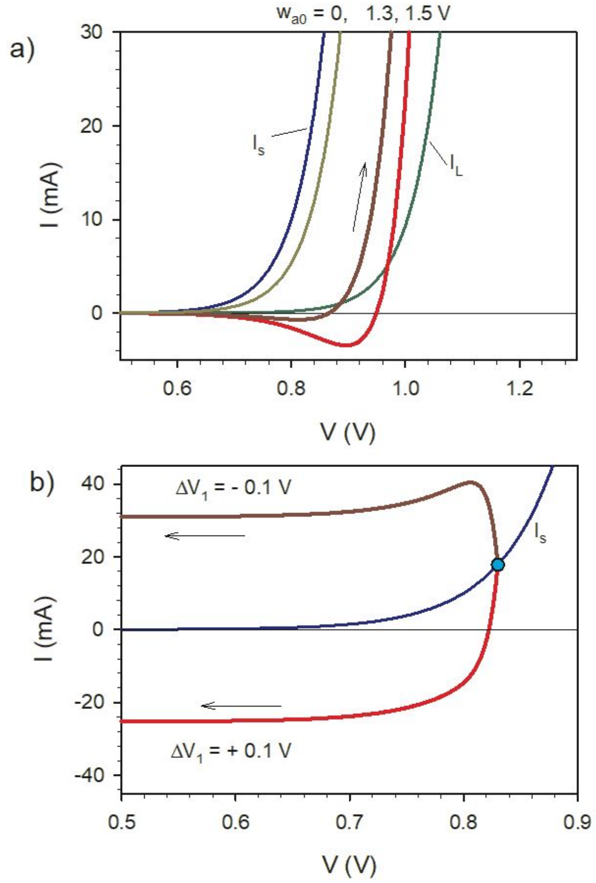

Fig. S2. Prepolarization of the inductive circuit. (a) Current-voltage curves at forward scan at different w_{a0} values for the parameters $R_{dc0} = 2.5 \times 10^4\ \Omega$, $R_{10} = 50/49\ R_{dc0}$, $R_{30} = 50\ R_{dc0}$, $\tau_k = 1$ s, $k_B T =\ 0.026$ V, $m = 2$, $V_m = 0.052$ V, $V_s = 1$ V/s. (b) Reverse scan at velocity $B_s = 0.01$ V/s starting at $V_1 = 0.83\ V$ (point) at positive and negative polarization.

2. IS Fit Parameters

Capacitive Circuit

Table S1. IS fit parameters using the capacitive equivalent circuit model for the MAPI and Triple Cation samples, with effective areas of 0.12 cm^2 and 0.295 cm^2, respectively measured under illuminated conditions.

Sample	Voltage (V)	R_3 ($\Omega \cdot cm^2$)	C_g ($F \cdot cm^{-2}$)	R_1 ($\Omega \cdot cm^2$)	C_1 ($F \cdot cm^{-2}$)
MAPI (Illuminated)	0.4	41.292	5.47×10^{-7}	784.8	0.006625
	0.5	36.984	6.17×10^{-7}	311.52	0.0090
	0.6	31.116	8.53×10^{-7}	198	0.01475
	0.7	23.784	6.22×10^{-7}	148.8	0.03008
	0.8	16.968	6.45×10^{-7}	102.012	0.067417
	0.9	9.8028	6.89×10^{-7}	36.576	0.21583
	1	3.3036	7.66×10^{-7}	4.3668	1.79325
TC (Illuminated)	0	33.4825	1.32×10^{-7}	769.95	0.000854
	0.2	35.046	9.64×10^{-8}	549.29	0.00063
	0.4	29.5295	1.13×10^{-7}	188.859	0.000674
	0.6	20.62345	1.02×10^{-7}	81.302	0.001215
	0.8	11.3988	7.14×10^{-8}	22.0306	0.002164
	1	6.8086	7.57×10^{-8}	3.5046	0.018233

Inductive Circuit

Table S2. IS fit parameters using the inductive equivalent circuit model for the MAPBr 0% RH sample, with an effective area of 0.237 cm^2, measured under dark conditions.

Sample	Voltage (V)	R_3 ($\Omega \cdot cm^2$)	C_g ($F \cdot cm^{-2}$)	R_a ($\Omega \cdot cm^2$)	L_a ($H \cdot cm^2$)
MAPBr 0% RH (Dark)	1.2	2655.348	1.71×10^{-7}	29710.32	5629.461
	1.3	359.292	1.31×10^{-7}	681.849	69.915
	1.4	67.4502	1.34×10^{-7}	160.8756	15.54246
	1.5	23.50329	7.62×10^{-8}	22.95345	1.58458
	1.6	12.61077	6.64×10^{-8}	6.95595	0.38465
	1.7	9.59139	5.60×10^{-8}	3.62136	0.18677

References

(1) Richardson, G.; O'Kane, S. E. J.; Niemann, R. G.; Peltola, T. A.; Foster, J. M.; Cameron, P. J.; Walker, A. B. Can slow-moving ions explain hysteresis in the current-voltage curves of perovskite solar cells?, *Energy Environ. Sci.* **2016**, *9*, 1476-1485.

(2) Nemnes, G. A.; Besleaga, C.; Tomulescu, A. G.; Palici, A.; Pintilie, L.; Manolescu, A.; Pintilie, I. How measurement protocols influence the dynamic J-V characteristics of perovskite solar cells: Theory and experiment, *Sol. Ener.* **2018**, *173*, 976-983.

(3) Nemnes, G. A.; Besleaga, C.; Tomulescu, A. G.; Leonat, L. N.; Stancu, V.; Florea, M.; Manolescu, A.; Pintilie, I. The hysteresis-free behavior of perovskite solar cells from the perspective of the measurement conditions, *J. Mat. Chem. C* **2019**, *7*, 5267-5274.

(4) Cao, X.; Li, Y.; Li, C.; Fang, F.; Yao, Y.; Cui, X.; Wei, J. Modulating Hysteresis of Perovskite Solar Cells by a Poling Voltage, *J. Phys. Chem. C* **2016**, *120*, 22784-22792.

(5) Ravishankar, S.; Almora, O.; Echeverría-Arrondo, C.; Ghahremanirad, E.; Aranda, C.; Guerrero, A.; Fabregat-Santiago, F.; Zaban, A.; Garcia-Belmonte, G.; Bisquert, J. Surface Polarization Model for the Dynamic Hysteresis of Perovskite Solar Cells, *J. Phys. Chem. Lett.* **2017**, 915-921.

(6) Lopez-Varo, P.; Jiménez-Tejada, J. A.; García-Rosell, M.; Ravishankar, S.; Garcia-Belmonte, G.; Bisquert, J.; Almora, O. Device Physics of Hybrid Perovskite Solar cells: Theory and Experiment, *Adv. Energy Mater.* **2018**, 1702772.

(7) Tress, W.; Marinova, N.; Moehl, T.; Zakeeruddin, S. M.; Nazeeruddin, M. K.; Gratzel, M. Understanding the rate-dependent J-V hysteresis, slow time component, and aging in CH3NH3PbI3 perovskite solar cells: the role of a compensated electric field, *Energy Environ. Sci.* **2015**, *8*, 995-1004.